REPORT 1236

ARRANGEMENT OF FUSIFORM BODIES TO REDUCE THE WAVE DRAG AT SUPERSONIC SPEEDS [1]

By Morris D. Friedman and Doris Cohen

SUMMARY

By means of linearized slender-body theory and reverse-flow theorems, the wave drag of a system of fusiform bodies at zero angle of attack and supersonic speeds is studied to determine the effect of varying the relative location of the component parts. The investigation is limited to two-body and three-body arrangements of Sears-Haack minimum-drag bodies. It is found that in certain arrangements the interference effects are beneficial, and may even result in the two- or three-body system having no more wave drag than that of the principal body alone. The most favorable location appears to be one in which the maximum cross-section of the auxiliary body is slightly forward of the Mach cone from the tail of the main body. The least favorable is the region between the Mach cone from the nose and the forecone from the tail of the main body.

INTRODUCTION

When an airplane is to be equipped with external fuel tanks or prominent nacelles, the effect on the drag will vary widely with the location of such auxiliary bodies relative to the other parts of the airplane. In reference 1, calculations were made of the theoretical interference drag between the fusiform bodies of some typical arrangements, under the conditions of supersonic speed and zero angle of attack. Later developments in linear theory have provided a simpler method of performing such calculations, and the present paper is a revision of reference 1 to take advantage of these developments. Both reference 1 and the present work are largely based on suggestions of R. T. Jones.

Two arrangements will be considered—a two-body combination, as when one body is suspended beneath another, and a laterally symmetric three-body arrangement. The radial and streamwise displacements of the auxiliary body or bodies relative to the main one will constitute the parameters of the investigation. The calculations will be made for combinations of Sears-Haack minimum-drag bodies (refs. 2 and 3), but the method of analysis is applicable to any slender shapes for which the pressure fields are known. In particular, it may be mentioned that the main body and auxiliary bodies need not be similar.

[1] Supersedes NACA RM A51I20, "Arrangement of Bodies of Revolution in Supersonic Flow to Reduce Wave Drag," by Morris D. Friedman, 1951, and NACA TN 3345, by Morris D. Friedman and Doris Cohen, 1954.

ANALYSIS

REVERSED-FLOW THEORY

A basic condition of the analysis is that the bodies be slender enough so that the resulting disturbance of an oncoming stream may be represented by a linear distribution of singularities—sources for a body of revolution, or higher-order singularities for cambered bodies—of which the strength may be determined from local conditions. In that case, simultaneously reversing the direction of flow and the sign of the source strength associated with a given isolated body does not change the shape of the body, and the reversed-flow theorems of reference 4, which are stated in terms of source distributions, may be applied to the bodies themselves. However, the streamlines at a distance from the body are altered, so that it is not generally to be expected that the theorems would be applicable to a *system* of bodies of prescribed geometry. The location of the individual bodies of the system in the streamlines of the other bodies has the effect of introducing additional camber into the boundary conditions and thereby modifying the equivalent distribution of singularities. Calculations made to investigate the effect of such induced camber on the drag of slender bodies indicate that the magnitude is not likely to be any significant fraction of the thickness drag.[2] The additional drag introduced by the induced camber will therefore be ignored. With this simplication, the drag of a system of slender bodies may be said to remain unchanged when the direction of motion is reversed.

In the present calculations, in which each of the bodies is symmetrical fore and aft, the first consequence of the reversibility property is that only rearward (or forward) displacements of the auxiliary bodies relative to the main body need be considered.

The reversibility property also leads to the possibility of combining the pressure fields for forward and reverse motion *before* computing the drag, and taking half the resulting drag as the drag in either direction. This point may be demonstrated as follows:

Regarding the body as stationary in an oncoming stream, let dR/dx be the local inclination of any element of surface

[2] For example, the drag due to parabolic camber of a line of sources corresponding to a Sears-Haack body is $\frac{16}{3}(M^2-1)h^2$ times the drag of the uncambered body, h being the maximum camber in percent of body length.

area dS (of a body of revolution) to the stream and c_{p_f} be the pressure coefficient at the centroid of the element (see fig. 1). Then the corresponding element of drag is simply (to the first order)

$$qc_{p_f}(dR/dx)\,dS$$

where q is the free-stream dynamic pressure and S is the surface area. Now, let the body be reversed on the x axis (fig. 2), with its tail headed into the relative wind. At the

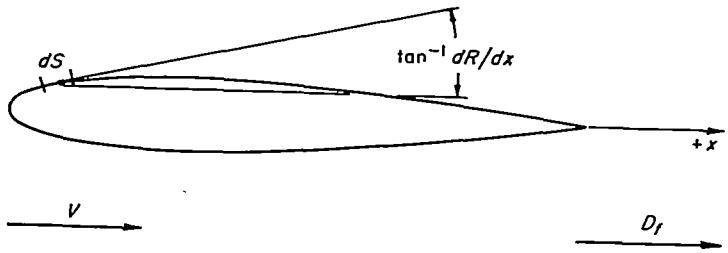

FIGURE 1.—Drag and relative wind corresponding to forward motion of the body.

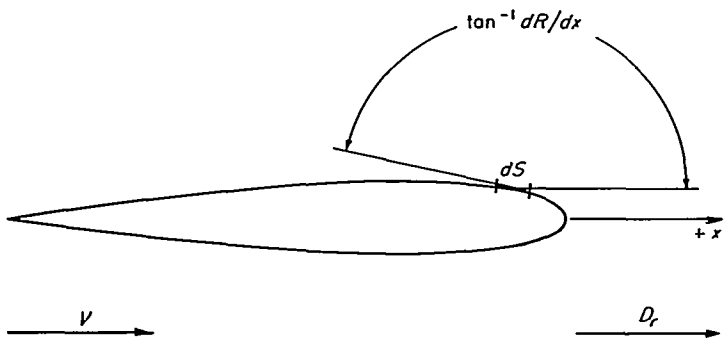

FIGURE 2.—Drag and relative wind in reverse flow.

previously considered element of area a new pressure coefficient c_{p_r} will result; the slope dR/dx will merely be reversed in sign. The sum of the two elements of drag will be

$$dD_f+dD_r=q(c_{p_f}-c_{p_r})\left(\frac{dR}{dx}\right)_f dS \tag{1}$$

where the subscript f refers to quantities corresponding to forward motion and r to rearward, or reverse flow. The total combined drag is the integral of this quantity, and is twice the drag of the body traveling in either direction.

The foregoing device, similar to one first suggested in reference 5, results in considerable mathematical simplification in many cases. Thus, the argument of reference 6 that in the combined flow field the drag of one wing due to the field of another is equal to that of the second due to the field of the first can be extended to apply to systems of slender bodies under the conditions outlined above. Then only one calculation of the interference drag need be made for each pair of bodies; for example, in the present analysis only the drag of the auxiliary body due to the combined pressure field $(c_{p_f}-c_{p_r})$ of the main body will be calculated.

PRESSURE FIELD OF A SEARS-HAACK BODY

In the examples to be worked in this paper, all bodies will be closed bodies of revolution having individually the form for minimum theoretical wave drag for given length and volume. This shape (refs. 2 and 3) is given by

$$R^2(x)=c(l^2-x^2)^{3/2} \tag{2}$$

(See Appendix for a list of symbols.) The flow about one such body can be calculated as the flow due to a distribution of sources and sinks along the body axis, the source strength $f(x)$ being related to the body geometry by the equation (ref. 7)

$$2\pi f(x)=V\frac{dS_c}{dx}=\pi V\frac{dR^2}{dx} \tag{3}$$

The pressure coefficient near the body is given to the first order (see ref. 8) by the relation

$$c_p=-\frac{2u}{V}-\left(\frac{v}{V}\right)^2 \tag{4a}$$

in which $u=\partial\varphi/\partial x$ is the streamwise component of the perturbation velocity and $v=\partial\varphi/\partial r$ the radial component. Inasmuch as the latter component falls off with distance from the body as $1/r$ and its contribution to the pressure decreases with $1/r^2$, it may be possible to neglect the second term in c_p in computing the interference drag. It will be shown by a numerical example that this simplification is in fact permissible in the present investigation. At the surface of the body, the ratio v/V is, to first order, the streamwise slope of the body and, in the case of the symmetrical bodies under consideration, the integration for the drag will result in canceling out all effects of the radial component of velocity. Thus it is sufficient for our purpose to retain only the linear term in equation (4a), writing

$$c_p\simeq-\frac{2u}{V} \tag{4b}$$

From reference 7,

$$\frac{\partial\varphi}{\partial x}=-\int_{nose}^{x-\beta r}\frac{f'(\xi)d\xi}{\sqrt{(x-\xi)^2-\beta^2r^2}} \tag{5}$$

From equations (2) and (3), $f'(\xi)$ is in the present case

$$-\frac{3}{2}Vc\frac{l^2-2\xi^2}{\sqrt{(l^2-\xi^2)}}$$

and

$$c_p\simeq-3c\int_{-l}^{x-\beta r}\frac{(l^2-2\xi^2)d\xi}{\sqrt{(l^2-\xi^2)[(x-\xi)^2-\beta^2r^2]}} \tag{6}$$

It should be remarked that for $\xi>l$ the integrand vanishes, and that c_p is zero when $x-\beta r<-l$.

The integration in equation (6) yields three different expressions, depending on whether

$$\beta r-l<x<l-\beta r \quad \text{(Region I)}$$

$$|l-\beta r|<x<l+\beta r \quad \text{(Region II)}$$

or

$$x>l+\beta r \quad \text{(Region III)}$$

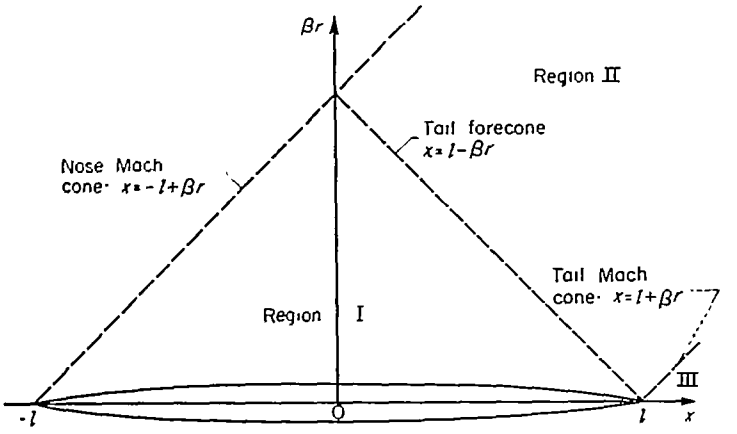

FIGURE 3.—Regions in pressure field around isolated Sears-Haack body.

The three regions defined above are shown in figure 3. The expressions for the approximate pressure coefficient are

Region I

$$c_{p_I}\simeq -3\pi c\left[\frac{l^2+2\beta r(l-x)-2x^2}{\sqrt{(l+\beta r)^2-x^2}}K_o(k_1)-\sqrt{(l+\beta r)^2-x^2}\,E_o(k_1)+2x\Lambda_o(\psi_1,k_1)\right]$$

$$k_1=\sqrt{\frac{(l-\beta r)^2-x^2}{(l+\beta r)^2-x^2}}\qquad \psi_1=\sin^{-1}\sqrt{\frac{l+\beta r+x}{2l}} \tag{7}$$

Region II

$$c_{p_{II}}\simeq -3\pi c\left[\frac{l(l+2\beta r-2x)}{2\sqrt{l\beta r}}K_o(k_2)-2\sqrt{l\beta r}\,E_o(k_2)+2x\Lambda_o(\psi_2,k_2)\right]$$

$$k_2=\sqrt{\frac{x^2-(\beta r-l)^2}{4l\beta r}}\qquad \psi_2=\sin^{-1}\sqrt{\frac{2l}{l+\beta r+x}} \tag{8}$$

Region III

$$c_{p_{III}}\simeq 3\pi c\left[\frac{(x-\beta r)^2}{\sqrt{x^2-(\beta r-l)^2}}K_o(k_3)+\sqrt{x^2-(\beta r-l)^2}E_o(k_3)-2x\Lambda_o(\psi_3,k_3)\right]$$

$$k_3=\sqrt{\frac{4l\beta r}{x^2-(\beta r-l)^2}}\qquad \psi_3=\sin^{-1}\sqrt{\frac{l+x-\beta r}{l+x+\beta r}} \tag{9}$$

The quantities K_o, E_o and Λ_o are defined in the Appendix and tabulated in reference 9; Λ_o is tabulated also in reference 10.

The magnitude of the approximate pressure coefficient, as given by equation (7), at the surface of a body of fineness ratio 10 at $M=\sqrt{2}$ is plotted in figure 4, together with the more accurate values obtained by the use of equation (4a). It is apparent that the difference, in the case of so slender a body, is not great and, as previously noted, will diminish rapidly with distance.

An isometric sketch of the pressure coefficient calculated by equations (7), (8), and (9) is shown in figure 5. Of particular interest is the logarithmic infinity along the Mach cone from the tail of the body. Except at the body itself, the pressure is finite everywhere else and goes smoothly

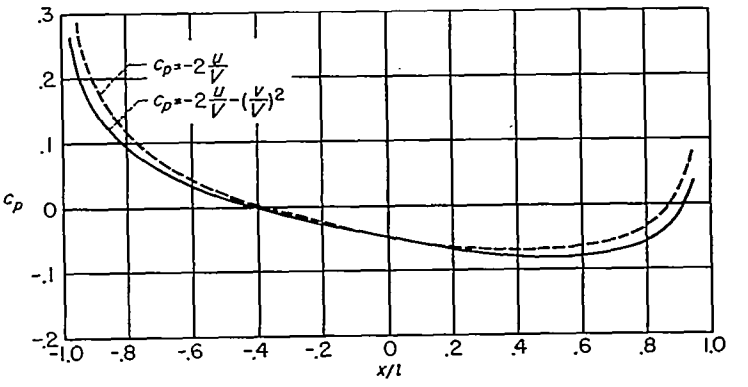

FIGURE 4.—Pressure coefficient on Sears-Haack body, fineness ratio 10, at $M=\sqrt{2}$. Effect of v^2 term.

through the forecone from the tail, in spite of the change in the form of its mathematical expression.

COMBINED PRESSURE FIELD

If now the body is reversed in heading and the resulting pressure field subtracted from that given above, the combined pressure field is found as

$$\bar{c}_p(x)=c_p(x)-c_p(-x) \tag{10}$$

because of the fore-and-aft symmetry of the body. The various regions of the combined field are shown in figure 6.

It is seen from figure 6 that there is only one region in which any possibility of further mathematical simplification appears. In this region (where Region I and Region I of the reversed field overlap) we have to consider

$$\bar{c}_{p_I}=c_{p_I}(x)-c_{p_I}(-x) \tag{11}$$

Through the relation (ref. 10, p. 36)

$$\Lambda_o(\psi,k)+\Lambda_o(\bar{\psi},k)=1+k'^2K_o\sin\psi\sin\bar{\psi}$$

when

$$\tan\psi\tan\bar{\psi}=\frac{1}{k}$$

equation (11) reduces to

$$\bar{c}_{p_I}=-6\pi cx \tag{12}$$

Thus, the pressure gradient of the combined field is a constant in the neighborhood of the body, as specified in reference 6 for minimum wave drag with a given volume.[3]

CALCULATION OF THE WAVE DRAG

As previously indicated, it is proposed in calculating the drag to ignore the drag introduced by the curvature of the flow due to adjacent bodies, and therefore to replace each body by the equivalent source distribution in a uniform stream. If, following this course, we consider the entire flow field to be essentially the result of the superposition of the fields of the individual bodies, we have to compute

(a) one-half the drag of each body in its own combined pressure field,

[3] Although reference 6 deals specifically with thin wings, it is readily shown that the same considerations hold for slender bodies under the assumptions used herein.

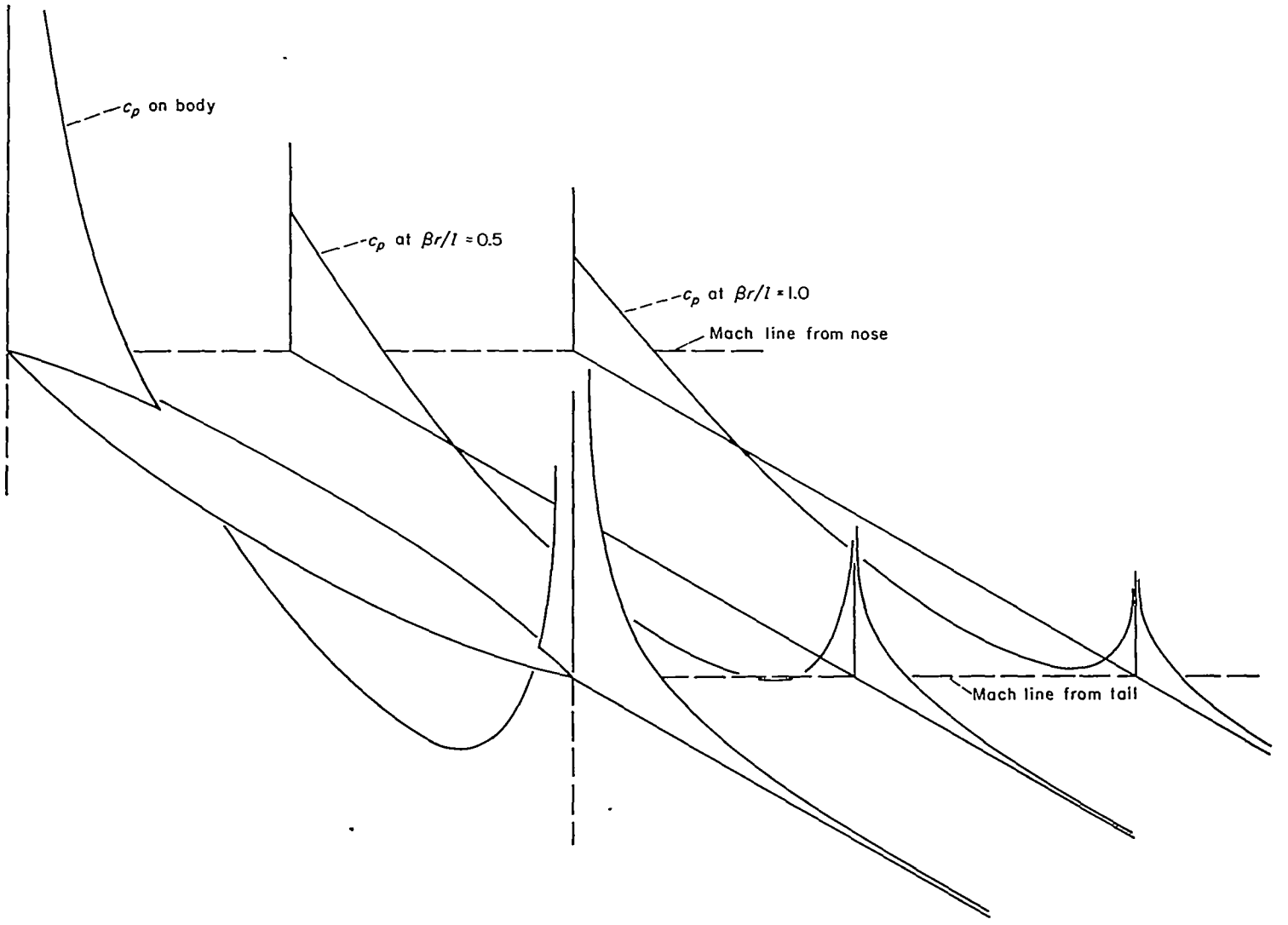

FIGURE 5.—Isometric sketch of the pressure distribution in the field surrounding a single Sears-Haack body, fineness ratio 10, at $M=\sqrt{2}$.

(b) the drag of each auxiliary body in the combined field of the main body, and

(c) the drag of one auxiliary body in the field of the other, if more than one auxiliary body is included. It may be seen that the drag of the second body in the field of the first is taken care of by the factor of 2 introduced by the use of the combined pressure field.

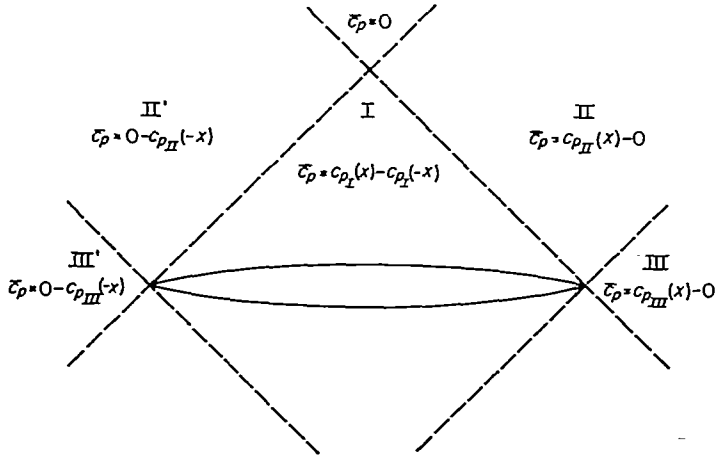

FIGURE 6.—Regions in combined pressure field of a single body.

If equation (1) is applied to a body of revolution, the total drag in combined flow may be written

$$\overline{D}=2\pi q\int_{-l}^{+l}\bar{c}_p R\frac{dR}{dx}\,dx=\pi q\int_{-l}^{+l}\bar{c}_p\frac{dR^2}{dx}\,dx \tag{13}$$

and, for the Sears-Haack bodies,

$$\frac{dR^2}{dx}=-3cx\sqrt{l^2-x^2} \tag{14}$$

The drag of each body due to its own pressure field is then one-half that obtained by substituting from equations (12) and (14) in equation (13), or

$$D_o=9\pi^2 qc^2\int_{-l}^{+l}x^2\sqrt{l^2-x^2}\,dx$$

$$=\frac{9}{8}\pi^3 ql^4c^2 \tag{15}$$

or, since the maximum cross-sectional area is, from equation (2),

$$S_F=\pi cl^3 \tag{16}$$

the drag in terms of frontal area is

$$D_o=\frac{9}{8}\pi\frac{S_F^2}{l^2}q \tag{17}$$

which is in agreement with the value given in reference 2.

The interference drag is calculated by substituting in equation (13) the pressure coefficient associated with one body and the value of dR^2/dx associated with the other. Considering first a two-body combination, we may take the origin of coordinates at the center of one, which will be designated the "main" body, and let the center of the auxiliary body be displaced from it a distance x_o downstream and a distance r_o laterally or vertically. Then, if for a first approximation the pressure field of the main body is assumed not to vary significantly in the distance between the axis of the auxiliary body and its surface, the values of $\bar{c}_p$ are obtained from equations (12), (8), and (9) by letting $r=r_o$. Equation (14) is modified to take into account the displacement of the auxiliary body:

$$\frac{dR^2}{dx}=-3c_1(x-x_0)\sqrt{l_1^2-(x-x_0)^2} \tag{18}$$

and the geometric characteristics of the second body are used to determine c_1 and l_1.

It is immediately apparent that if the auxiliary body lies entirely within Region I (fig. 6), the value of $\bar{c}_p$, and therefore of the drag, is independent of r_o. In fact, since the pressure gradient is a constant throughout the region, the drag is entirely independent of position so long as the body remains within Region I. The interference drag in this case is simply

$$D_1=\frac{9}{8}\pi^3 q l_1^4 c c_1 \tag{19}$$

or, more generally, D_1/q equals the pressure gradient $6\pi c$ times the volume of the auxiliary body, regardless of its shape. It follows that, since the interference drag cannot be reduced by redistributing the additional volume within this region, the Sears-Haack body remains the optimum auxiliary body for this configuration, regardless of interference effects.[4] It is possible that in a region of more rapidly changing pressure gradient a significantly different shape for minimum drag would be found.

In Region II the pressure gradient changes from negative to positive (see fig. 5) and a small body placed so as to take advantage of this buoyancy would conceivably experience a negative interference drag, or thrust, which would act to reduce the total drag of the combination. Substitution of $c_{p_{II}}$ and, when required, $c_{p_{III}}$ in equation (13) results in integrals which can be evaluated only numerically. We therefore proceed at this point to the consideration of numerical examples.

NUMERICAL CALCULATIONS

For an exploratory investigation, the simple case of two bodies of fineness ratio 10, the small body having one-half the length of the main body, was chosen. With the half-length of the larger body taken as unity, the other parameters of the problem were

$$l_1=\tfrac{1}{2}$$

$$c=0.01$$

$$c_1=0.02$$

In compressible flow, the Mach number and cross-stream dimensions enter together in the form βr. The investigation covered values of $\beta r_o/l$ ranging from 0.25 to 1.4. The effect of streamwise displacement of the centers was explored to a distance equal to the length of the larger body.

The interference between the two outer bodies of a three-body configuration was calculated in the case of $\beta r_o/l=0.25$ (assuming the distance between the smaller bodies to be double the distance of each from the main body) and the effect on the drag was found to be negligible. The results to be presented are therefore equally applicable to the two-body or three-body arrangement, only a factor of 2 in the interference drag being required.

RESULTS AND DISCUSSION

The variation of interference drag with streamwise and radial displacement is shown in figures 7 and 8. Because of the symmetry of the curves, only the region to the rear of the main body is shown. The anticipated favorable interference is observed when the small body is situated astride the region of negative pressure gradient just ahead of the Mach wave from the stern of the large body, the benefit of course decreasing with increasing radial separation of the bodies. The corresponding forward location of the small body would be equally favorable, in accordance with the reciprocity principle, because of the buoyancy imparted to the large body by the wave from the stern of the small one. The maximum drag is incurred when the auxiliary body is added in the region enclosed by the Mach cone from the nose of the main body and the Mach forecone from its tail. Further outboard of this region, in line with the maximum cross-section of the large body and just forward of the Mach cone from its nose, is a second, small region of favorable interference, where the pressure field of the large body acts only on the rear of the small body, and vice versa, resulting in unopposed thrust.

In figure 8 the sketches indicate, for $M=\sqrt{2}$, the relative positions of the bodies when the interference is greatest. The situation last described is shown at $x_0=0$ in figure 8 (c). From this point, or the low slightly further outboard of it (fig. 7), areas of reduced drag extend both ways in directions generally parallel to the Mach lines. That running from upper left to lower right in the figure results from the action of the bow wave from the small body on the rear of the large one; that in the opposite direction results from the bow wave of the large body pushing on the rear of the small one. The lowest drag of all results from the coincidence of one of these areas with the negative-drag area associated with the shock wave at the stern.

In figures 9 and 10 the wave drag coefficient based on total frontal area is shown for two-body and three-body arrange-

[4] An investigation by Rennemann (ref. 11) of a similar interference problem, with main body *parabolic* in shape, but with the location of the auxiliary body similarly restricted to Region I, indicates an optimum auxiliary body whose form and added drag differ only slightly from those of a Sears-Haack body.

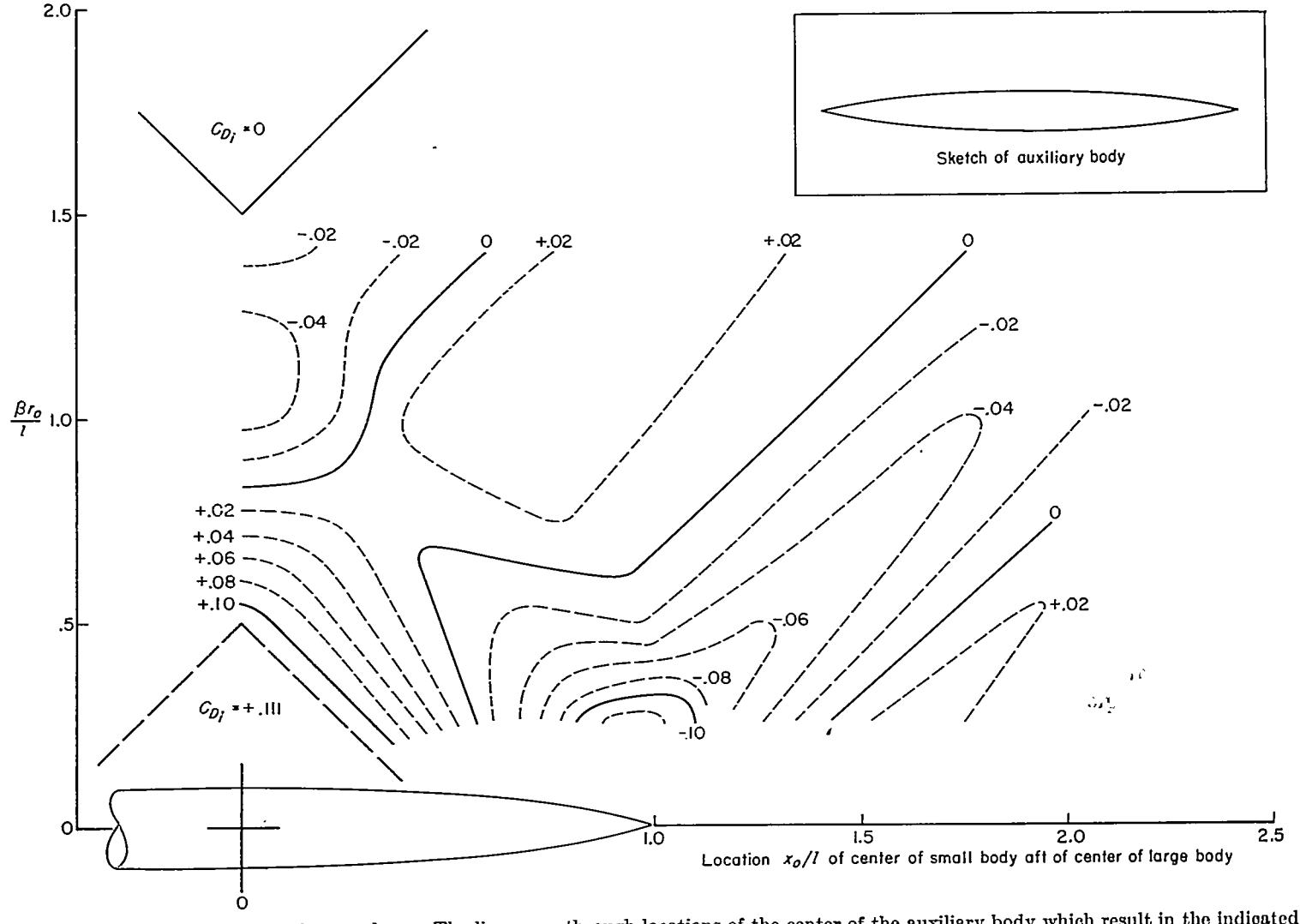

FIGURE 7.—Contour lines of interference drag. The lines pass through locations of the center of the auxiliary body which result in the indicated values of interference drag per unit added frontal area.

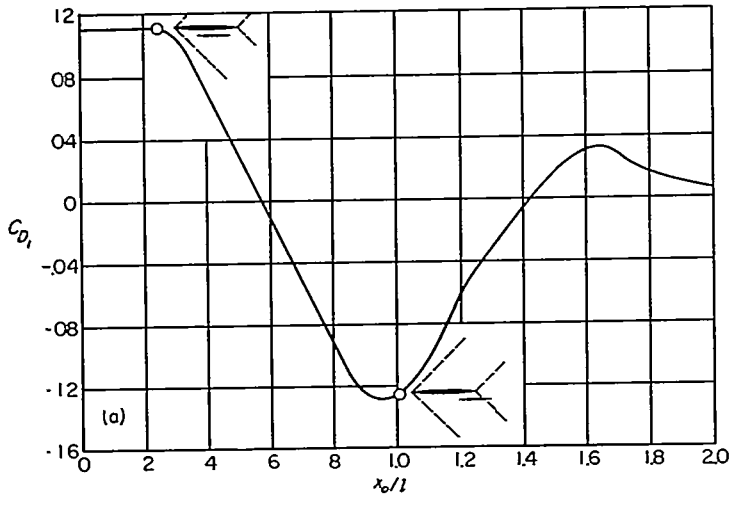

(a) $\beta r_o/l = 0.25$

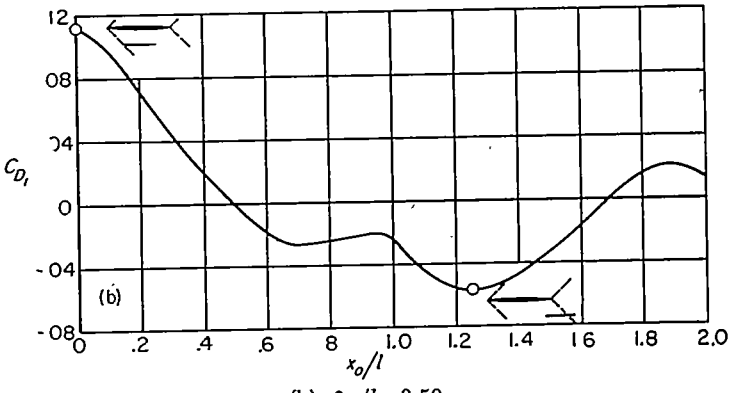

(b) $\beta r_o/l = 0.50$

FIGURE 8.—Interference drag per unit added frontal area.

FIGURE 8.—Continued.

ments. In connection with figure 10 it may be noted that the bodies need not be side by side as shown. If the small bodies are suspended below the wing, the distance between

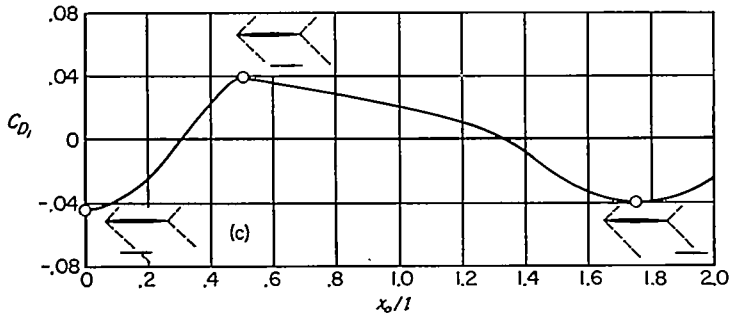

(c) $\beta r_o/l = 1.00$

FIGURE 8.—Concluded.

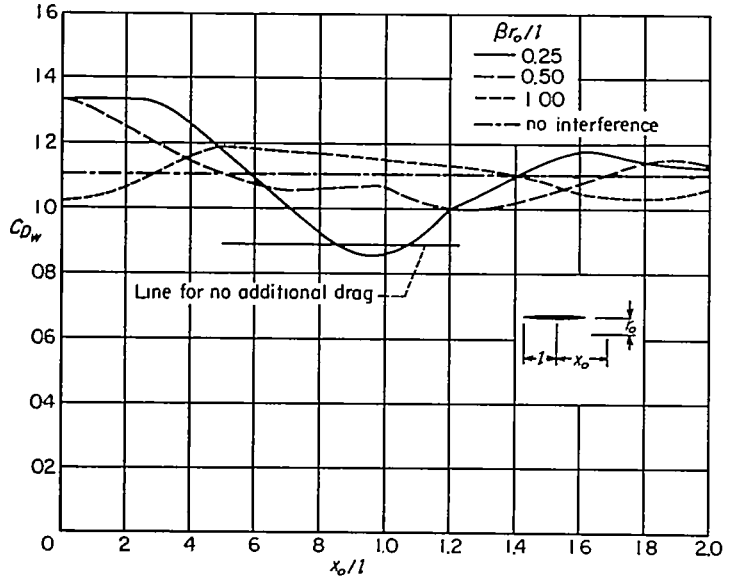

FIGURE 9.—Wave-drag coefficient of two-body systems based on total frontal area.

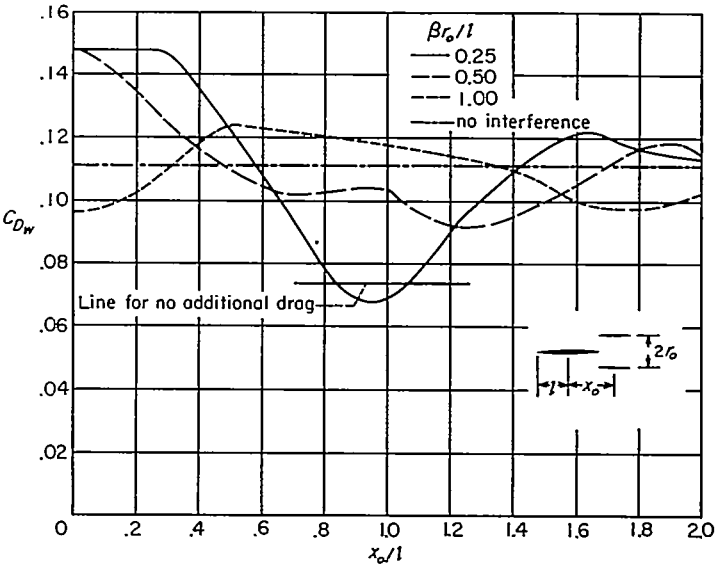

FIGURE 10.—Wave-drag coefficient of three-body systems based on total frontal area.

them may be less than $2r_o$. However, the results shown will still apply as long as the bodies are not so close as to give rise to appreciable additional interference drag.

Figures 9 and 10 indicate that in frictionless potential flow it might be possible to increase the volume by as much as 25 percent (three-body arrangement) and at the same time actually decrease the wave drag. In practice, of course, the additional friction drag might easily nullify any such gain. Nevertheless, if there are to be auxiliary bodies, the importance of a careful selection of their relative positions seems clear.

AMES AERONAUTICAL LABORATORY
NATIONAL ADVISORY COMMITTEE FOR AERONAUTICS
MOFFETT FIELD, CALIF., *September 8, 1954*

APPENDIX

SYMBOLS

c	coefficient containing body dimensions, $\frac{R^2_{max}}{l^3}$
c_1	value of c for auxiliary body
C_{D_W}	wave-drag coefficient, $\frac{D_W}{qS_F}$
C_{D_i}	interference drag coefficient, $\frac{D_i}{qS_F}$
c_p	local pressure coefficient
c_{p_f}	pressure coefficient in forward motion
c_{p_r}	pressure coefficient in reversed motion
$\overline{c}_p$	pressure coefficient in "combined" field, $c_{p_f}-c_{p_r}$
D_W	wave drag
D_o	wave drag of isolated body
D_i	interference drag
D_f	wave drag in forward motion
D_r	wave drag in reversed motion
$\overline{D}$	combined wave drag, D_f+D_r
E_o	$\frac{2}{\pi}$ times complete elliptic integral of the second kind
f	source strength
k	modulus of elliptic integrals (with subscripts to indicate different values)
k'	complementary modulus, $\sqrt{1-k^2}$
K_o	$\frac{2}{\pi}$ times complete elliptic integral of the first kind
l	half-length of body
l_1	half-length of auxiliary body
M	free-stream Mach number
q	free-stream dynamic pressure
r	radial coordinate, measured from body axis
r_o	radial coordinate of center of auxiliary body, measured from axis of main body
R	local radius of body (function of x)
R_{max}	radius of body at maximum cross section
S	surface area
S_c	cross-sectional area
S_F	maximum cross section, or frontal area
u	streamwise component of perturbation velocity
v	radial component of perturbation velocity
V	free-stream velocity
x	streamwise coordinate, origin at the center of body
x_o	streamwise coordinate of center of auxiliary body, measured from center of main body
β	$\sqrt{M^2-1}$
$\Lambda_o(\psi,k)$	Heumann's elliptic function, $E_o(k)F(\psi,k')+K_o(k)E(\psi,k')-K_o(k)F(\psi,k')$, tabulated in references 9 and 10
ξ	streamwise coordinate of source, origin at center of body
φ	perturbation velocity potential
ψ	argument of incomplete elliptic integrals in Λ_o (with subscripts to denote various values)

REFERENCES

1. Friedman, Morris D.: Arrangement of Bodies of Revolution in Supersonic Flow to Reduce Wave Drag. NACA RM A51I20, 1951.
2. Sears, William R.: On Projectiles of Minimum Wave Drag. Quart. Appl. Math., vol. IV, No. 4, Jan. 1947, pp. 361–366.
3. Haack, W.: Projectile Shapes for Smallest Wave Drag. Brown Univ., Grad. Div. Appl. Math., Trans. A9–T–3, 1948.
4. Hayes, Wallace D.: Linearized Supersonic Flow. (Thesis) North Amer. Aviation, Inc., Rep. AL–222, 1947.
5. Munk, M. M.: The Reversal Theorem of Linearized Supersonic Airfoil Theory. Jour. Appl. Phys., vol. 21, No. 2, Feb. 1950, pp. 159–161.
6. Jones, Robert T.: Theoretical Determination of the Minimum Drag of Airfoils at Supersonic Speeds. Jour. Aero. Sci., vol. 19, No. 12, Dec. 1952, pp. 813–822.
7. von Kármán, Th.: The Problem of Resistance in Compressible Fluids. GALCIT pub. No. 75, 1936. (From R. Acad. D'Italia; cl. scie., fis. mat. e nat., vol. XIV, 1936.)
8. Lighthill, M. J.: Methods for Predicting Phenomena in the High-Speed Flow of Gases. Jour. Aero. Sci., vol. 16, No. 2, Feb. 1949, pp. 69–83.
9. Heumann, Carl: Tables of Complete Elliptic Integrals. Jour. Math. and Phys., vol. 19–20, 1940–41, pp. 127–206.
10. Byrd, Paul F., and Friedman, Morris D.: Handbook of Elliptic Integrals for Engineers and Physicists. Springer-Verlag (Berlin), 1954.
11. Rennemann, Conrad, Jr.: Minimum-Drag Bodies of Revolution in a Non-Uniform Supersonic Flow Field. NACA TN 3369, 1955.